

Nature of Driven Cavity Flow at High-Re and Benchmark Solutions on Fine Grid Mesh

E. Erturk

*Energy Systems Engineering Department, Gebze Institute of Technology
Gebze, Kocaeli 41400, Turkey*

SUMMARY

The numerical solutions of 2-D steady incompressible flow in a driven cavity are presented. The Navier-Stokes equations in streamfunction and vorticity variables are solved simply with Successive Over Relaxation (SOR) method. Using a very fine grid mesh with 1025×1025 points, the steady driven cavity flow is solved for $Re \leq 20,000$. For accuracy, the iterations are carried out on the streamfunction and vorticity variables until the steady streamfunction and vorticity equations are satisfied with a residual that were less than 10^{-10} . Interesting features of the flow are presented in detail. The nature of the driven cavity flow at high Reynolds numbers is discussed in detail in terms of physical and mathematical and also numerical aspects, in an attempt to address the controversy on this flow problem at high Reynolds numbers.

KEY WORDS: Steady 2-D Incompressible N-S Equations; Cavity Flow; Fine Grid Solutions; High Reynolds Numbers

1. INTRODUCTION

The lid driven cavity flow is most probably one of the most studied fluid problems in computational fluid dynamics field. The simplicity of the geometry of the cavity flow makes the problem easy to code and apply boundary conditions and etc. Even though the problem looks simple in many ways, the flow in a cavity retains all the flow physics with counter rotating vortices appear at the corners of the cavity.

The driven cavity flow has been studied very extensively and it is possible to find many papers on this flow problem in the literature. Driven cavity flow serve as a benchmark problem and almost every new numerical method for the 2-D steady incompressible Navier-Stokes equations are tested on the driven cavity flow in terms of accuracy, numerical efficiency and

Email: ercanerturk@gyte.edu.tr

Download figures, tables, data files, fortran codes and etc. from <http://www.cavityflow.com>. All the numerical solutions presented in this study is available to public in this web site.

Contract/grant sponsor: GYTE-BAP; contract/grant number: BAP-2003-A-22

etc. However, even though the driven cavity flow is studied at this extent, the nature of the flow at high Reynolds number is still not agreed upon. For this flow there is a controversy at high Reynolds numbers such that some studies predict that the flow is steady, some predict that the flow is not steady but is time dependent. Among many numerical studies on driven cavity flow, Erturk et. al. [12], Barragy & Carey [4], Schreiber & Keller [36], Benjamin & Denny [6], Liao & Zhu [27], Ghia et. al. [20] have presented solutions of *steady* 2-D incompressible flow in a driven cavity for $Re \leq 10,000$. Among these, Barragy & Carey [4] have also presented solutions for $Re=12,500$. The controversy got even bigger when Erturk et. al. [12] have presented steady solutions up to $Re=21,000$. On the other hand, many studies claimed that the 2-D incompressible flow in a cavity is *unsteady* and a steady solution does not exist beyond some Reynolds numbers. These studies will be discussed later on in detail.

The main purpose of this study is then to present very fine grid steady solutions of the driven cavity flow at very high Reynolds numbers. Based on the results obtained a brief discussion about the physical, mathematical and numerical nature of an incompressible flow in a 2-D driven cavity will be done together with a very brief literature survey, in an attempt to address the controversy on this flow problem.

2. PROBLEM FORMULATION AND NUMERICAL ALGORITHM

First, as the starting point, we assume that the incompressible flow in a driven cavity is *two-dimensional*. A second point is that, we are seeking a *steady* solution. After these two starting points, the problem at hand is governed by the 2-D steady incompressible Navier-Stokes equations. We use the governing equations in streamfunction (ψ) and vorticity (ω) formulation such that

$$\frac{\partial^2 \psi}{\partial x^2} + \frac{\partial^2 \psi}{\partial y^2} = -\omega \quad (1)$$

$$\frac{1}{Re} \left(\frac{\partial^2 \omega}{\partial x^2} + \frac{\partial^2 \omega}{\partial y^2} \right) = \frac{\partial \psi}{\partial y} \frac{\partial \omega}{\partial x} - \frac{\partial \psi}{\partial x} \frac{\partial \omega}{\partial y} \quad (2)$$

These equations are non-dimensional, where Re is the Reynolds number, and x and y are the Cartesian coordinates.

The above equations are solved with a very well known numerical method, the Successive Over Relaxation (SOR) method. SOR method is most probably the simplest and the most easy to apply numerical method. For this flow problem, the solver is less than 30 lines of Fortran code. The solution methodology is quite simple. First an initial guess is assigned to $\psi_{i,j}$ and $\omega_{i,j}$ where i and j are the grid index in x- and y-direction respectively. As an initial guess either a homogeneous solution can be used or alternatively for a given Reynolds number, a previously obtained smaller Reynolds number solution can be used. The grids are numbered from 0 to N where N is the number of grids points. Same number of grid points is used in x- and y-directions. Then in a nested loop of

DO $i=1,N-1$

DO $j=1,N-1$

the streamfunction variable is advanced using the following equation

$$\psi_{i,j}^{n+1} = \beta \left(0.25(\psi_{i-1,j}^{n+1} + \psi_{i,j-1}^{n+1} + \psi_{i+1,j}^n + \psi_{i,j+1}^n + h^2 \omega_{i,j}) \right) + (1 - \beta) \psi_{i,j}^n \quad (3)$$

where h is the grid spacing ($\Delta x = \Delta y = h$) and β is the relaxation parameter. The streamfunction value at the wall is zero.

The vorticity values at the wall is calculated using Jensen's formula (see Fletcher [15])

$$\omega_0 = \frac{-4\psi_1 + 0.5\psi_2}{h^2} - \frac{3V}{h} \quad (4)$$

where subscript 0 refers to the points on the wall and 1 refers to the points adjacent to the wall and 2 refers to the second line of points adjacent to the wall and also V refers to the velocity of the wall with being equal to 1 on the moving wall and 0 on the stationary walls. Then similarly, in a nested loop

DO $i=1, N-1$

DO $j=1, N-1$

the vorticity variable is advanced using the following equations

$$\omega_{i,j}^{n+1} = \beta \left(0.25 \left(\omega_{i-1,j}^{n+1} + \omega_{i,j-1}^{n+1} + \omega_{i+1,j}^n + \omega_{i,j+1}^n - 0.25 \operatorname{Re}(\psi_{i,j+1} - \psi_{i,j-1})(\omega_{i+1,j}^n - \omega_{i-1,j}^{n+1}) \right. \right. \\ \left. \left. + 0.25 \operatorname{Re}(\psi_{i+1,j} - \psi_{i-1,j})(\omega_{i,j+1}^n - \omega_{i,j-1}^{n+1}) \right) \right) + (1 - \beta) \omega_{i,j}^n \quad (5)$$

During the iterations, as a measure of the convergence to the steady state, we monitored three residual parameters. The first residual parameter, RES1, is defined as the maximum absolute residual of the finite difference equations of steady streamfunction and vorticity equations (1 and 2). These are respectively given as

$$\operatorname{RES1}_\psi = \max \left(\left| \frac{\psi_{i-1,j}^{n+1} - 2\psi_{i,j}^{n+1} + \psi_{i+1,j}^{n+1}}{h^2} + \frac{\psi_{i,j-1}^{n+1} - 2\psi_{i,j}^{n+1} + \psi_{i,j+1}^{n+1}}{h^2} + \omega_{i,j}^{n+1} \right| \right) \\ \operatorname{RES1}_\omega = \max \left(\left| \frac{1}{\operatorname{Re}} \frac{\omega_{i-1,j}^{n+1} - 2\omega_{i,j}^{n+1} + \omega_{i+1,j}^{n+1}}{h^2} + \frac{1}{\operatorname{Re}} \frac{\omega_{i,j-1}^{n+1} - 2\omega_{i,j}^{n+1} + \omega_{i,j+1}^{n+1}}{h^2} \right. \right. \\ \left. \left. - \frac{\psi_{i,j+1}^{n+1} - \psi_{i,j-1}^{n+1}}{2h} \frac{\omega_{i+1,j}^{n+1} - \omega_{i-1,j}^{n+1}}{2h} + \frac{\psi_{i+1,j}^{n+1} - \psi_{i-1,j}^{n+1}}{2h} \frac{\omega_{i,j+1}^{n+1} - \omega_{i,j-1}^{n+1}}{2h} \right| \right) \quad (6)$$

We think that among the three residual parameters, RES1 is the most important residual parameters. The magnitude of RES1 is an indication of the degree to which the solution has converged to steady state. In the limit RES1 would be zero.

The second residual parameter, RES2, is defined as the maximum absolute difference between two iteration steps in the streamfunction and vorticity variables. These are respectively given as

$$\operatorname{RES2}_\psi = \max (| \psi_{i,j}^{n+1} - \psi_{i,j}^n |)$$

$$\text{RES2}_\omega = \max (|\omega_{i,j}^{n+1} - \omega_{i,j}^n|) \quad (7)$$

RES2 gives an indication of the significant digit on which the code is iterating.

The third residual parameter, RES3, is similar to RES2, except that it is normalized by the representative value at the previous time step. This then provides an indication of the maximum percent change in ψ and ω in each iteration step. RES3 is defined as

$$\begin{aligned} \text{RES3}_\psi &= \max \left(\left| \frac{\psi_{i,j}^{n+1} - \psi_{i,j}^n}{\psi_{i,j}^n} \right| \right) \\ \text{RES3}_\omega &= \max \left(\left| \frac{\omega_{i,j}^{n+1} - \omega_{i,j}^n}{\omega_{i,j}^n} \right| \right) \end{aligned} \quad (8)$$

Note that, when a homogeneous initial guess is used, then in the first iteration, calculation of RES3 is skipped since $\psi_{i,j}$ and $\omega_{i,j}$ is homogeneous. During iterations, there is always a chance that $\psi_{i,j}$ and/or $\omega_{i,j}$ could get a value of zero making RES3 indeterminate. However since a double precision is used, it is almost impossible for $\psi_{i,j}$ and $\omega_{i,j}$ to get exact value of 0.00...00, although the chance remains. Anyhow, we choose to use RES3 in our code in order to have an idea about the percent change in the streamfunction and vorticity variable at each iteration.

In our calculations, for all Reynolds numbers we considered that convergence was achieved when both $\text{RES1}_\psi \leq 10^{-10}$ and $\text{RES1}_\omega \leq 10^{-10}$ was achieved. Such a low value was chosen to ensure the accuracy of the solution. At these convergence levels the second residual parameters were in the order of $\text{RES2}_\psi \leq 10^{-17}$ and $\text{RES2}_\omega \leq 10^{-15}$, that means the streamfunction and vorticity variables are accurate to 16th and 14th digit accuracy respectively at a grid point and even more accurate at the rest of the grids. Also at these convergence levels the third residual parameters were in the order of $\text{RES3}_\psi \leq 10^{-14}$ and $\text{RES3}_\omega \leq 10^{-13}$, that means the streamfunction and vorticity variables are changing with 10⁻¹²% and 10⁻¹¹% of their values respectively in an iteration step at a grid point and even with less percentage at the rest of the grids. Obviously these convergence levels are far more less than satisfactory and one would think that such low values are not necessary. One of the reasons why we let the iterations converge to these levels was to demonstrate that for the driven cavity flow even a basic SOR algorithm is capable of achieving such low residual values at high Reynolds numbers when a fine grid mesh is used. During the iterations the three residual parameters steadily decrease without any oscillations.

The number of grid points used in this study is 1025×1025 .

3. RESULTS

The boundary conditions and a schematics of the vortices generated in a driven cavity flow are shown in Figure 1 In this figure, the abbreviations BR, BL and TL refer to bottom right, bottom left and top left corners of the cavity, respectively. The number following these abbreviations refer to the vortices that appear in the flow, which are numbered according to size. Lately Erturk et. al. [12] have presented an efficient numerical method and with using their numerical method they have presented steady solutions of the cavity flow up to Reynolds number of 21,000

using fine grid mesh. They have clearly stated that in order to obtain a steady solutions at high Reynolds numbers ($Re > 10,000$), a grid mesh larger than 257×257 have to be used. We have decided to test the validity of their statement using SOR algorithm. The SOR algorithm is an explicit algorithm and it is most probably the easiest algorithm in terms of coding. First we start with a grid mesh of 257×257 . With this many grid points we could not obtain a solution for Reynolds numbers above 10,000 no matter how small we choose the relaxation parameters. Then we increased the number of grids to 513×513 . This time we were able to obtain steady solutions up to $Re \leq 15,000$. With using this many number of grids, one thing is important to note, at Reynolds number of 17,500 when sufficiently small relaxation parameters were used such that the code did not diverged, the solution was not converging but it was oscillating. Erturk et. al. [12] have obtained the same type of behavior when they were using a coarse grid mesh. They stated that when they increased the number of grids used, they were able to obtain a converged solution. In this study, we then decided to increase the number of grids to 1025×1025 . This time we were able to obtain converged steady solutions up to Reynolds number of 20,000. We note that with this many number of grids we could not obtain a solution for 21,000 as Erturk et. al. [12] have obtained. The solution at $Re = 21,000$ was oscillating again when sufficiently small relaxation parameters were used. This suggests that most probably, when a larger grid mesh is used the steady computations are possible.

For a given Reynolds number, we have used the same β values for both streamfunction and vorticity equations (3 and 5) and these β values are tabulated in Table 1. We note that we did not try to obtain the optimum β values at a given Reynolds number that would offer the fastest convergence. What we did was, when the solution diverged we decreased the value of β by 0.1.

Figure 2 and Figure 3 show the streamfunction and vorticity contours of the cavity flow up to $Re \leq 20,000$ with 1025×1025 grid mesh. These contour figures show that, the fine grid mesh provides very smooth solutions at high Reynolds numbers.

The location of the primary and the secondary vortices and also the streamfunction (ψ) and vorticity (ω) values at these locations are tabulated in Table 2. These results are in good agreement with Erturk et. al. [12]. They have stated that they have observed the quaternary vortex at the bottom left corner, BL3, appear in the solution at $Re = 10,000$ when fine grids (600×600) were used. In this study we found that, when a more fine grid mesh (1025×1025) is used, BL3 vortex appear in the solution at $Re = 7,500$. This would then suggest that in order to resolve the flow at high Reynolds numbers, fine grids are necessary.

Figure 4 and 5 show the u-velocity distribution along a vertical line and the v-velocity along a horizontal line passing through the center of the cavity respectively, at various Reynolds numbers. Detailed quantitative results obtained using a fine grid mesh was tabulated extensively in Erturk et. al. [12], therefore quantitative tabulated results will not be repeated in this study. The results obtained in this study agrees well with Erturk et. al. [12] and the reader is referred to that study for quantitative results. The reason why we choose to plot the u- and v-velocity profiles in Figures 4 and 5 is that, since the considered flow in cavity is incompressible we can use these velocity profiles to test the accuracy of the solution. If there exists a solution to the 2-D steady incompressible equations at high Reynolds numbers, then this solution must satisfy the continuity of the fluid. The continuity will provide a very good mathematical check on the solution as it was suggested first by Aydin & Fenner [3]. As seen in Figures 4 and 5 the integration of these velocity profiles will give the plus and minus areas shown by grey colors. The degree to which the plus and minus areas cancel each other

such that the integration gives a value close to zero, will be an indicative of the mathematical accuracy of the solution. The velocity profiles are integrated using Simpson's rule to obtain the net volumetric flow rate Q passing through these sections. The obtained volumetric flow rates are then normalized by a characteristic flow rate, $Q_c = 0.5$, which is the horizontal rate that would occur in the absence of the side walls (Plane Couette flow), to help quantify the errors. The obtained volumetric flow rate values ($Q_1 = \frac{|\int_0^1 u dy|}{Q_c}$ and $Q_2 = \frac{|\int_0^1 v dx|}{Q_c}$) are tabulated in Table 3. The volumetric flow rates in Table 3 are so small that they can be considered as $Q_1 \approx Q_2 \approx 0$. This mathematical check on the conservation of the continuity shows that our numerical solution is indeed very accurate.

4. DISCUSSIONS

Based on the studies we found in the literature, we conclude that there are some confusions on the subject of driven cavity flow. We think that, the flow problem has three aspects; physical (hydrodynamic), mathematical and numerical (computational) aspects and also the problem has to be analyzed in terms of these aspects *separately*.

We would like to note that a very brief discussion on computational and also experimental studies on driven cavity flow can be found on Shankar & Deshpande [37]. In this study, the literature and also the discussion is presented from a perspective trying to address the controversy on the nature of the flow in a driven cavity at high Reynolds numbers. First let us analyze the physical aspects of the cavity flow and look at the experimental studies.

Koseff & Street [24, 25, 26], Prasad & Koseff [32] have done several experiments on three dimensional driven cavity with various spanwise aspect ratios (SAR). Their experiments ([24, 25, 26, 32]) have shown that the flow in a cavity exhibits both local and global three-dimensional features. For example in a local sense they have found that Taylor-Goertler-Like (TGL) vortices form in the region of the Downstream Secondary Eddy (DSE). Also corner vortices form at the cavity end walls. In a global scale, due to no slip boundary condition on the end walls the flow is three-dimensional. They ([24, 25, 26, 32]) concluded that two-dimensional cavity flow does not exist (up to SAR=3) and further more, the presence of the TGL vortices precludes the possibility that the flow will be two dimensional even at large SAR. These conclusions clearly show that a two dimensional approximation for the flow in a cavity breaks down physically even at moderate Reynolds numbers.

Their results ([24, 25, 26, 32]) have also shown that the flow is laminar but unsteady even at moderate Reynolds numbers. The flow starts to show the signs of turbulence characteristics with turbulent bursts between $6,000 \leq Re \leq 8,000$. Above Reynolds number of 8,000 the flow in a cavity is turbulent (for SAR=3).

According to these valuable physical information provided by [24, 25, 26, 32], the fact of the matter is, the flow in cavity is neither two-dimensional nor steady at high Reynolds numbers. Since two-dimensional steady flow in a cavity at high Reynolds numbers do not occur in reality, this flow (ie. 2-D steady cavity flow at high Re) is a fictitious flow, as also concluded by Shankar & Deshpande [37]. This is a very important fact to remember.

In our computations, as a starting point we have assumed that the flow inside a cavity is two-dimensional, therefore, we have used the 2-D Navier-Stokes equations. We numerically solve these equations for different Reynolds numbers and all of the obtained solutions are based

on the assumption that the flow is two-dimensional. At this point we should ask the question "Could an incompressible flow inside a cavity be two-dimensional at high Reynolds numbers?". Let us consider a 3-D cavity with a moderate spanwise aspect ratio (SAR). In this cavity, as the Reynolds number increases up to some Reynolds numbers the flow at the symmetry plane (at the center in z-axis) could be assumed two dimensional. However after some Reynolds number the walls in third dimension (z-direction) will start to affect the flow due to non-slip condition (end-wall-effects). Above these Reynolds numbers, physically, the flow inside this cavity can not be assumed two dimensional. If we use a different cavity with a larger aspect ratio, still, after some Reynolds number the third dimensional effects cannot be ignored and a 2-D assumption fails after these Reynolds numbers. Now let us assume that hypothetically we have a cavity with an infinite aspect ratio ($SAR \rightarrow \infty$), then in terms of the end-wall-effects, only in this case the flow can be assumed purely two dimensional at any Reynolds numbers, and this is a fictitious scenario. We note that, here we look at the cavity flow only on a global scale and consider only the end-wall-effects. As explained in [24, 25, 26, 32] and also in some computations that will be mentioned later on, in local scale TGL vortices appear in the region of the downstream secondary eddy (DSE). Therefore, even the flow in an infinite aspect ratio cavity will not be two-dimensional in reality.

Now let us analyze the cavity flow mathematically and also numerically. In our computations, we have used 2-D Navier stokes equations, and also we have presented *steady* solutions of the cavity flow at high Reynolds numbers. In light of these two points, what could be the nature of the flow at high Reynolds numbers? Mathematically speaking a two-dimensional flow cannot be turbulent. Turbulence is by nature three-dimensional and is not steady. Therefore due to our two-dimensional assumption, mathematically the flow could not be turbulent. Since, when 2-D equations are used and therefore we do not let the flow be turbulent mathematically, could the flow still be time dependent, ie. periodic? Although 2-D high Reynolds number scenario is fictitious, this is a legitimate question in terms of a mathematical and numerical analysis. At this point we are trying to answer the mathematical and numerical nature of a fictitious flow and see if there exists a steady solution to 2-D Navier-Stokes equations or not. Mathematically speaking, a two-dimensional flow can be either steady (ie. solution is independent of time) or unsteady but time dependent (ie. solution is periodic in time) or unsteady but time independent (ie. solution is completely chaotic). Since, mathematically speaking, there is a possibility that the flow could be either steady or unsteady, then is the flow in cavity steady or unsteady, or in other words does a steady solution exists to 2-D Navier-Stokes equations or not? In the literature it is possible to find studies that present steady solutions of 2-D incompressible Navier-Stokes equations at high Reynolds numbers such as Erturk et. al. [12], Barragy & Carey [4], Schreiber & Keller [36], Benjamin & Denny [6], Liao & Zhu [27], Ghia et. al. [20]. In the literature there are also studies that claims the cavity flow is unsteady. In these studies, researchers have tried to obtain the Reynolds number at which a Hopf bifurcation occurs in the flow, ie. Reynolds number at which the flow changes from steady to unsteady characteristics. These studies can be basically grouped into two categories. 1) In the first type of studies, the 2-D unsteady Navier-Stokes equations are solved via Direct Numerical Simulation (DNS). In these the Reynolds number is gradually increased and the time history of the solution is observed. When the solution of DNS converge to a steady solution, researchers claim that at these Reynolds numbers the flow inside a cavity is stable. At higher Reynolds numbers when the DNS solution do not converge to a steady state, the researchers conclude that the flow is unstable, ie the flow is not steady. In these studies the time behavior of the solution above a

Hopf bifurcation Reynolds numbers is also analyzed. 2) In the second type of studies the basic steady cavity flow solution is perturbed with small disturbances and then the eigenvalues of linearized Navier-Stokes equations are analyzed via hydrodynamic stability analysis. We will discuss the second type of studies later on, but first let us look at the first type of studies that have used DNS, in detail.

Auteri, Parolini & Quartepelle [2] have used a second order spectral projection method. With this they have solved the Unsteady 2-D N-S equations in primitive variables. They have analyzed the stability of the driven cavity with an impulsively started lid using 160×160 grids. They have removed the singularity that occurs at the corners of the cavity. They have increased the Reynolds number step by step until the solution becomes periodic. They have found that a Hopf bifurcation occurs in the interval $Re = 8,017.6-8,018.8$. At this Reynolds number their solution was periodic with a frequency of 0.4496. They also reported that the cavity flow passes through a second Hopf bifurcation in the interval $Re = 9,687-9,765$.

Peng, Shiau & Hwang [29] have used a Direct Numerical Simulation (DNS) by solving the 2-D unsteady Navier-Stokes equations in primitive variables. With using a maximum of 200×200 grids, they have solved the cavity flow by increasing the Reynolds number. At $Re = 7,402 \pm 4$ their solutions became periodic with a certain frequency of 0.59. As Re was increased to 10,300 the flow became a quasi-periodic regime. When the Re was increased to 10,325 the flow returned to a periodic regime again. Between Reynolds numbers of 10,325 and 10,700 the flow experienced an inverse period doubling and between 10,600 and 10,900 the flow experienced a period doubling. Finally they claimed that the flow becomes chaotic when Re was greater than 11,000.

Tiesinga, Wubs & Veldman [41] have used Newton-Picard method and recursive projection method using a 128×128 grid mesh and with these they claimed that in a 2-D incompressible flow inside a cavity the first a Hopf bifurcation occurs at $Re = 8,375$ with a frequency of 0.44. The next Hopf bifurcations occur at $Re = 8,600, 9,000, 9,100$ and $10,000$ with frequencies 0.44, 0.53, 0.60 and 0.70. At these intervals the flow is either stable periodic or unstable periodic.

Poliashenko & Aidun [31] have used a direct method based on time integration. Using Newton iterations with 57×57 number of grid points they have claimed that a Hopf bifurcation occurs in a lid driven cavity at $Re = 7,763 \pm 2\%$ with a frequency of $2.86 \pm 1\%$. They have stated that this Hopf bifurcation is supercritical.

Cazemier, Verstappen & Veldman [8] have used Proper Orthogonal Decomposition (POD) and analyzed the stability of the cavity flow. They compute the first 80 POD modes, which on average capture 95% of the fluctuating kinetic energy, from 700 snapshots that are taken from a Direct Numerical Simulation (DNS). They have stated that the first Hopf bifurcation take place at $Re = 7,819$ with a frequency of about 3.85.

Goyon [21] have solved 2-D unsteady Navier-Stokes equations in streamfunction and vorticity variables using Incremental Unknowns with a maximum mesh size of 257×257 . They have stated that a Hopf bifurcation appears at a critical Reynolds number between 7,500 to 10,000. They have presented periodic asymptotic solutions for $Re = 10,000$ and 12,500.

Wan, Zhou & Wei [43] have solved the 2-D incompressible Navier-Stokes equations with using a Discrete Singular Convolution method on a 201×201 grid mesh. Also Liffman [28] have used a Collocation Spectral Solver and solved the 2-D incompressible Navier-Stokes with 64×64 collocation points. Both studies claimed that the flow in a cavity is periodic at Reynolds number of 10,000.

These are just example studies we picked from the literature that uses Direct Numerical

Simulation (DNS) to capture the critical Reynolds number that a Hopf bifurcation occurs in a driven cavity flow.

In order to obtain numerical simulations of 2-D incompressible flows, the Navier-Stokes equations can either be considered in primitive variable formulation or in streamfunction and vorticity formulation. In the following statements, we mainly concentrate on the streamfunction and vorticity formulation of the Navier-Stokes equations, however similar statements can be made for the primitive variable formulation also. 2-D Steady Incompressible Navier-Stokes equations are elliptic equations. In general, in terms of numerical solution methodology, there are three ways of numerically solving the elliptic equations, ie. the 2-D steady incompressible Navier-Stokes equations in streamfunction and vorticity formulation:

1) One way is to solve the governing equations as they are and use elliptic type of iterative numerical methods for the solution of these equations. Then the governing Navier-Stokes equations are considered for the numerical solution in the following form

$$\frac{\partial^2 \psi}{\partial x^2} + \frac{\partial^2 \psi}{\partial y^2} = -\omega \quad (9)$$

$$\frac{1}{\text{Re}} \left(\frac{\partial^2 \omega}{\partial x^2} + \frac{\partial^2 \omega}{\partial y^2} \right) = \frac{\partial \psi}{\partial y} \frac{\partial \omega}{\partial x} - \frac{\partial \psi}{\partial x} \frac{\partial \omega}{\partial y} \quad (10)$$

These equations are then solved numerically using Jacobi iteration or Gauss-Seidel iteration or Successive Over Relaxation (SOR) or line iteration or red-black scheme or etc. (see Tennehill, Anderson & Pletcher [40] and Fletcher [15]).

2) Second way is to assign pseudo time derivatives to the governing equations and solve the equations in this pseudo time domain. The obtained equations are then parabolic in the pseudo time, such that parabolic type of iterative numerical methods can be used. The governing equations are in the following form

$$\frac{\partial \psi}{\partial t} = \frac{\partial^2 \psi}{\partial x^2} + \frac{\partial^2 \psi}{\partial y^2} + \omega \quad (11)$$

$$\frac{\partial \omega}{\partial t} = \frac{1}{\text{Re}} \left(\frac{\partial^2 \omega}{\partial x^2} + \frac{\partial^2 \omega}{\partial y^2} \right) - \frac{\partial \psi}{\partial y} \frac{\partial \omega}{\partial x} + \frac{\partial \psi}{\partial x} \frac{\partial \omega}{\partial y} \quad (12)$$

These equations are then solved using any type of time stepping algorithm. We note that in this approach the time history of streamfunction and vorticity variables do not have any physical meaning, since physically the streamfunction equation is not time dependent. Note that when the solution converges to a steady state, in both equations the pseudo time derivative terms become equal to zero and drops out from the equations. Therefore the steady solution is obtained.

3) Third way is to use the physical time dependent equations. The equations are in the following form

$$\frac{\partial^2 \psi}{\partial x^2} + \frac{\partial^2 \psi}{\partial y^2} = -\omega \quad (13)$$

$$\frac{\partial \omega}{\partial t} = \frac{1}{\text{Re}} \left(\frac{\partial^2 \omega}{\partial x^2} + \frac{\partial^2 \omega}{\partial y^2} \right) - \frac{\partial \psi}{\partial y} \frac{\partial \omega}{\partial x} + \frac{\partial \psi}{\partial x} \frac{\partial \omega}{\partial y} \quad (14)$$

These equations are then solved via a DNS (Direct Numerical Simulation) algorithm. Again note that when the solution converges to a steady state the time derivative in the vorticity equation become homogeneous and the steady solution is obtained.

The advantages or disadvantages of these three numerical approaches and also numerical stability and any type of numerical issues are not our concern at the moment. We will be concentrating only on the numerical approach. Let us imagine that the 2-D incompressible flow inside a cavity is not stable at a given Reynolds number, such that a steady solution does not exist and the solution is time dependent. In this case, if the first numerical approach is used, one should not obtain a solution since there is no steady state. In this case, if the solution in time is desired then only the third approach has to be used, cause the time solution of the second approach has no physical meaning. Now let us imagine the opposite, such that, the 2-D incompressible flow inside a cavity is stable at a given Reynolds number. In this case the flow is steady and a steady solution does exist. If one uses the first numerical approach and obtain a numerical solution, then the second and third approaches should converge to this solution through iterations in time also. In all the three approaches, the boundary conditions are the same and these boundary conditions are independent of time. Therefore if there exist a unique solution to the first approach then the second and third approaches should converge to this solution also, since there is nothing to drive the solution vary in time because the boundary conditions are steady and also a steady solution of governing equations exists. If they (the second and third approaches) do not converge to this solution then this would mean that there are numerical stability issues with these approaches and the time dependent periodic solution or any other solution obtained that is different than the steady solution should not be trusted.

In this study we have used the first approach and obtained a steady solutions of driven cavity flow up to Reynolds number of 20,000. In an other study Erturk et. al. [12] have used the second approach and obtained steady solutions up to $Re=21,000$. Therefore, one should be able to obtain a steady solution when the third approach is used.

Erturk et. al. [12] have clearly stated that at high Reynolds numbers when they have used a grid mesh of 257×257 , they have observed that their solutions oscillate in the pseudo time. However, when they have used a larger grid mesh than 257×257 , they were able to obtain a steady solution at these high Reynolds numbers. In this study, when we have used a grid mesh of 257×257 , the solution did not converge to a steady solution at high Reynolds numbers also, even when very small relaxation parameters (β) were used, the solution was oscillating. But when we have increased the grid mesh to 513×513 we were able to obtain steady solutions up to $Re=15,000$. With this many number of grid points, above this Reynolds number, the solution started to oscillate again when sufficiently small relaxation parameters that would not allow the solution to diverge were used. And when we have increased the grid points up to 1025×1025 , we were able to obtain steady solutions up to $Re=20,000$. Therefore based on the experiences of Erturk et. al. and this study, we conclude that in order to obtain a steady solution for the driven cavity flow a grid mesh larger than 257×257 is necessary, when high Reynolds numbers are considered. We believe that, a Direct Numerical Simulation (DNS) would also converge to the same results obtained in this study and in Erturk et. al. [12] when larger grid meshes are used. Our very detailed literature survey showed that, in all the numerical studies of driven cavity flow, above Reynolds number of 5,000, the maximum number of grid points used is 257×257 . Larger grid meshes have never been used in studies above $Re=5,000$. As Erturk et. al. [12] have stated, one of the reasons, why the steady solutions of the driven cavity flow at very high Reynolds numbers become computable when finer grids are used, may be the fact that as the number of grids used increases, Δh gets smaller, then the cell Reynolds number or so called Peclet number defined as $Re_c = \frac{u\Delta h}{\nu}$ decreases. This improves the numerical stability characteristics of the numerical scheme used ([40, 44]), and allows high

cavity Reynolds number solutions computable. Another reason may be that fact that finer grids would resolve the corner vortices better. This would, then, help decrease any numerical oscillations that might occur at the corners of the cavity during iterations.

The interesting thing is that, both in this study and in Erturk et. al. [12], the obtained false periodic numerical solutions looked so real and fascinating with a certain frequencies and periodicity, even though the these periodic oscillations have no physical meaning since in these studies, first and second approaches were used respectively. We believe that the studies that presented unsteady solutions using Direct Numerical Simulations, [2, 29, 41, 31, 8, 21, 43, 28], have experienced the same type of numerical oscillations because they have used a small grid mesh. As we mentioned, these oscillations looks so real that they could easily be mistaken deceptively as real time behavior of the flow field. One may think that if the numerical simulation of time dependent equations (DNS) do not converge to steady state, then the flow is not hydrodynamically stable. However one should not forget that a DNS is also restricted with certain numerical stability conditions, such as a Peclet number restriction in driven cavity flow as explained in this study. We believe that DNS should not be used to predict the transition Reynolds number or Hopf bifurcation Reynolds numbers in a flow field, and if this is done the results obtained should not be trusted. Any numerical oscillations due to numerical stability issues can easily be confused as the hydrodynamic oscillations. In this context, numerical stability is not equivalent with hydrodynamic stability and should be confused with each other.

Now let us examine the studies that conclude the cavity flow is unsteady after doing a hydrodynamic stability analysis. Both external and internal flows, as Reynolds number is increased, exhibit a change from laminar to turbulent flow. In order to determine the Reynolds number that the transition from laminar to turbulent flow occurs, we use the Stability Theory. According to Stability Theory, in investigating the stability of laminar flows, the flow is decomposed into a basic flow whose stability is to be examined and a superimposed perturbation flow. The basic flow quantities are steady and the perturbation quantities vary in time. These basic and perturbation variables are inserted into Navier-Stokes equations. Assuming that the perturbations are small, equations are linearized and using a normal mode form for these perturbations, an Orr-Sommerfeld type of equation is obtained. The stability of a laminar flow becomes an eigenvalue problem of the ordinary differential perturbation equation. If the sign of imaginary part of the complex eigenvalue smaller than zero then the flow is stable, if it is greater than zero the flow is unstable (see Schlichting & Gersten [35] and also Drazin & Reid [11]).

In the case of driven cavity flow, the stability analysis requires solving the partial differential eigenvalue problem. Fortin et. al. [18], Gervais et. al. [19], Sahin & Owens [34] and Abouhamza & Pierre [1] are examples of hydrodynamic stability studies on driven cavity flow found in the literature. In these studies ([18, 19, 34, 1]), a two-dimensional basic flow is considered and then the solution of this two-dimensional basic flow is obtained numerically. Then this solution is perturbed with two-dimensional disturbances. The perturbation problem at hand is a partial differential eigenvalue problem, therefore the eigenvalues are also obtained numerically. These studies predict that a Hopf bifurcation takes place in a 2-D incompressible flow in a driven cavity some where around Reynolds number of 8,000.

One important point is that, the accuracy of the solution of the perturbation equation (or eigenvalues) completely depend on the accuracy of the solution of the basic flow. Since the perturbation quantities are assumed to be small compared to the basic flow quantities,

any negligible numerical errors will greatly affect the solution of the perturbation equation (Haddad & Corke [22], Erturk & Corke [13], Erturk et. al. [14]). Therefore for the sake of the accuracy of the solution of the perturbation equations, a highly accurate basic flow solution is required. In hydrodynamic analysis studies of driven cavity flow ([18, 19, 34, 1]) the number of grid points used is $\leq 257 \times 257$. This means that, the numerical solutions of the basic flow considered in these studies are restricted with Peclet number in terms of numerical stability. We note that the Hopf bifurcation predicted in these studies are close to Reynolds number limits of numerical stability for a maximum of 257×257 grid mesh. We believe that since a coarse grid is used in these studies, when the Reynolds number of the basic flow gets closer to numerical stability limits (ie. maximum stable Reynolds number for a given grid mesh), the numerical solution of the basic flow affects the perturbation analysis. Aside from this fact, since the eigenvalues are determined numerically, the eigenvalues themselves will also be a function of the grid spacing, ie. Δh .

Most importantly, a hydrodynamic analysis would only be useful and also meaningful when there exists a physical flow. Let us use another very well known fictitious flow as an example to make clear this point. The 2-D incompressible flow over a circular cylinder is steady for Reynolds number up to approximately 40. Beyond that Reynolds number there appears Karman vortex street at downstream of the cylinder and the physical ie. the real flow is unsteady. A steady solution beyond $Re=40$, if exists, is fictitious. However for this flow case, the 2-D incompressible flow over a cylinder, it is possible to obtain a steady solution mathematically when Re goes to infinity as the limiting solution (Kirchoff-Helmholtz solution, see Schlichting & Gersten [35]). This mathematical solution is useful in many ways, however does not reflect the physical behavior of the flow. Smith [38] and Peregrine [30] have done a detailed mathematical analysis on this fictitious flow at Reynolds numbers higher than 40. Fornberg [16, 17], Son & Hanratty [39], Tuann & Olson [42] and Dennis & Chang [9] have presented numerical solutions of steady flow past a circular cylinder at $Re=300, 600, 500, 100$ and 100 respectively, which are much larger than Reynolds number of 40. This fact is important such that, even though the flow is physically fictitious, a mathematical solution exists and also it is possible to obtain a numerical solution as well. Based on this example, since the steady flow over a circular cylinder at $Re>40$ is fictitious, there will not be a point to do a study that examine the hydrodynamic stability of the numerical solution of the flow over a cylinder, for example, at $Re=600$, by perturbing the basic flow solution and then solving the eigenvalue system at this Reynolds number numerically. Even though a study like this could be done, the results of such a study will be useless. The same is also true for the cavity flow. The experiments of Koseff & Street [24, 25, 26] and Prasad & Koseff [32] have shown that the flow inside a cavity is neither two-dimensional nor steady even at moderate Reynolds numbers. Therefore the results of a strictly two-dimensional hydrodynamic analysis (two-dimensional basic flow with two-dimensional perturbations) of a fictitious cavity flow will be also fictitious and will have no physical meaning.

Apart from the studies that examine the hydrodynamic stability of the driven cavity flow by considering a two-dimensional basic flow perturbed with two-dimensional disturbances mentioned above, the studies of Ramanan & Homsy [33] and Ding & Kawahara [10] are quite interesting and important. Both studies have considered a two-dimensional flow for driven cavity and analyzed when this two-dimensional basic flow is perturbed with three-dimensional disturbances. Ramanan & Homsy [33] found that the two dimensional flow loses stability at $Re=594$ when perturbed with three-dimensional disturbances, where as Ding & Kawahara

[10] have predicted the instability at $Re=1025$ with a frequency of 0.8. We believe that the results of Ding & Kawahara [10] greatly over estimates the critical Reynolds number since they have used a slight compressibility in their simulations, such that their results are not purely incompressible. Note that these critical Reynolds numbers are much lower than the strictly two-dimensional hydrodynamic analysis ([18, 19, 34, 1]). This is very important such that, the results of Ramanan & Homsy [33] and Ding & Kawahara [10] show that, for the stability of driven cavity flow the spanwise modes are more dangerous than the two dimensional modes. Also note that, their results ([33, 10]) do not include the effect of the end walls in spanwise direction. We expect that with including the effect of end walls and the TGL vortices, a three-dimensional flow analysis will have a lower critical Reynolds number for stability when perturbed with three-dimensional disturbances.

At this point the study of Kim & Moin [23] is noteworthy to mention. They have numerically simulated the three-dimensional time dependent flow in a square cavity with using periodic boundary conditions in the spanwise direction. They have observed TGL vortices in the flow field even though they did not have end walls in their simulations. Their results are important in the fact that in driven cavity flow the TGL vortices do not even need end walls to initiate.

5. CONCLUSIONS

In this study, the steady 2-D Navier-Stokes equations in streamfunction and vorticity formulation are solved numerically simply with using Successive-Over-Relaxation (SOR) algorithm. The lid driven cavity flow is definitely computable at high Reynolds numbers when a fine grid mesh is used, as stated by Erturk et. al. [12]. The solutions with using a 1025×1025 mesh showed that the quaternary vortex at the bottom left corner, BL3, appear in the solution at $Re=7,500$. Both the numerical residuals and also the mathematical continuity check prove that the presented numerical solutions are indeed very accurate.

After all the detailed discussions about the physical, mathematical and numerical characteristics of the incompressible flow in a driven cavity, we conclude the followings.

1. Physically, the flow in a driven cavity is not two dimensional and is not steady, most probably, even at $Re=1000$.
2. At high Reynolds numbers when the incompressible flow in a square cavity is considered as two-dimensional and also steady, then the considered flow is a fictitious flow.
3. It would be meaningless to study the hydrodynamic stability of a fictitious flow such as the two-dimensional incompressible cavity flow, especially when perturbed with two-dimensional disturbances.
4. Direct Numerical Simulation (DNS) should not be used in obtaining the hydrodynamic stability (ie. the critical Reynolds number) of a fluid flow problem.
5. Mathematically, it is always possible to obtain a steady solution of a fictitious flow at the limiting case when Re goes to infinity. As shown in Erturk et. al. [12], Bachelor's [5] model of recirculating flow confined in closed streamlines at infinite Reynolds number seems to work with the square driven cavity flow. The numerical solutions of Erturk et. al. [12] agrees well with the analytical solutions of Burggraf [7]. This analytical solution does not have a physical meaning.
6. Numerically, it is possible to obtain numerical solutions of 2-D steady incompressible

cavity flow at high Reynolds numbers when fine grid meshes are used. These solutions do not also have a physical meaning.

7. The model flow problem, the 2-D steady incompressible driven cavity flow can, still, serve as a good benchmark problem for different numerical methods and boundary conditions, in terms of accuracy, convergence rate and etc., provided that these numerical solutions should only be used for numerical comparison purposes between different solutions or with the analytical solution. The presented solutions in this study and the solutions of Erturk et. al. [12] provide high accurate, fine grid benchmark solutions for future references.

ACKNOWLEDGEMENT

This study was funded by Gebze Institute of Technology with project no BAP-2003-A-22. E. Ertürk is grateful for this financial support.

REFERENCES

1. A. Abouhamza and R. Pierre, A Neutral Stability Curve for Incompressible Flows in a Rectangular Driven Cavity, *Mathematical and Computer Modelling* **38** (2003) 141–157.
2. F. Auteri, N. Parolini and L. Quartapelle, Numerical Investigation on the Stability of Singular Driven Cavity Flow, *J. Comp. Physics* **183** (2002) 1–25.
3. M. Aydin and R.T. Fenner, Boundary Element Analysis of Driven Cavity Flow for Low and Moderate Reynolds Numbers, *Int. J. Numer. Methods Fluids* **37** (2001) 45–64.
4. E. Barragy and G.F. Carey, Stream Function-Vorticity Driven Cavity Solutions Using p Finite Elements, *Computers and Fluids* **26** (1997) 453–468.
5. G.K. Batchelor, On Steady Laminar Flow with Closed Streamlines at Large Reynolds Numbers, *J. Fluid Mech.* **1** (1956) 177–190.
6. A.S. Benjamin and V.E. Denny, On the Convergence of Numerical Solutions for 2-D Flows in a Cavity at Large Re, *J. Comp. Physics* **33** (1979) 340–358.
7. O.R. Burggraf, Analytical and Numerical Studies of the Structure of Steady Separated Flows, *J. Fluid Mech.* **24** (1966) 113–151.
8. W. Cazemier, R.W.C.P. Verstappen and A.E.P. Veldman, Proper Orthogonal Decomposition and Low-Dimensional Models for the Driven Cavity Flows, *Physics of Fluids* **10** (1998) 1685–1699.
9. S.C.R. Dennis and G-Z. Chang, Numerical Solutions for Steady Flow Past a Circular Cylinder at Reynolds Numbers up to 100, *J. Fluid Mech.* **42** (1970) 471–489.
10. Y. Ding and M. Kawahara, Linear Stability of Incompressible Fluid Flow in a Cavity Using Finite Element Method, *Int. J. Numer. Methods Fluids* **27** (1998) 139–157.
11. P.G. Drazin and W.H. Reid, *Hydrodynamic Stability* Cambridge University Press, 1991.
12. E. Erturk, T.C. Corke and C. Gokcol, Numerical Solutions of 2-D Steady Incompressible Driven Cavity Flow at High Reynolds Numbers, *Int. J. Numer. Methods Fluids* (2004) Submitted.
13. E. Erturk and T.C. Corke, Boundary layer leading-edge receptivity to sound at incidence angles, *J. Fluid Mech.* **444** (2001) 383–407.
14. E. Erturk, O.M. Haddad and T.C. Corke, Numerical Solutions of Laminar Incompressible Flow Past Parabolic Bodies at Angles of Attack, *AIAA J.* (2004) Accepted for publication.
15. C.A.J. Fletcher, *Computational Techniques for Fluid Dynamics* (2nd edn), Springer-Verlag, 1991.
16. B. Fornberg, A Numerical Study of Steady Viscous Flow Past a Circular Cylinder, *J. Fluid Mech.* **98** (1980) 819–855.
17. B. Fornberg, Steady viscous ow past a circular cylinder up to Reynolds number 600, *J. Comp. Phys.* **61** (1985) 297–320.
18. A. Fortin, M. Jardak, J.J. Gervais and R. Pierre, Localization of Hopf Bifurcations in Fluid Flow Problems, *Int. J. Numer. Methods Fluids* **24** (1997) 1185–1210.

19. J.J. Gervais, D. Lemelin and R. Pierre, Some Experiments with Stability Analysis of Discrete Incompressible Flows in the Lid-Driven Cavity, *Int. J. Numer. Methods Fluids* **24** (1997) 477–492.
20. U. Ghia, K.N. Ghia and C.T. Shin, High-Re Solutions for Incompressible Flow Using the Navier-Stokes Equations and a Multigrid Method, *J. Comp. Physics* **48** (1982) 387–411.
21. O. Goyon, High-Reynolds Number Solutions of Navier-Stokes Equations Using Incremental Unknowns, *Computer Methods in Applied Mechanics and Engineering* **130** (1996) 319–335.
22. O.M. Haddad and T.C. Corke, Boundary layer receptivity to free-stream sound on parabolic bodies, *J. Fluid Mech.* **368** (1998) 1–26.
23. J. Kim and P. Moin, Application of a Fractional-Step Method to Incompressible Navier-Stokes Equations, *J. Comp. Physics* **59** (1985) 308–323.
24. J.R. Koseff and R.L. Street, The Lid-Driven Cavity Flow: A Synthesis of Qualitative and Quantitative Observations, *ASME Journal of Fluids Engineering* **106** (1984) 390–398.
25. J.R. Koseff and R.L. Street, On End Wall Effects in a Lid Driven Cavity Flow, *ASME Journal of Fluids Engineering* **106** (1984) 385–389.
26. J.R. Koseff and R.L. Street, Visualization Studies of a Shear Driven Three-Dimensional Recirculating Flow, *ASME Journal of Fluids Engineering* **106** (1984) 21–29.
27. S.J. Liao and J.M. Zhu, A Short Note on Higher-Order Streamfunction-Vorticity Formulation of 2-D Steady State Navier-Stokes Equations, *Int. J. Numer. Methods Fluids* **22** (1996) 1–9.
28. K. Liffman, Comments on a Collocation Spectral Solver for the Helmholtz Equation, *J. Comp. Physics* **128** (1996) 254–258.
29. Y-H. Peng, Y-H. Shiau and R.R. Hwang, Transition in a 2-D Lid-Driven Cavity Flow, *Computers and Fluids* **32** (2003) 337–352.
30. D.H. Peregrine, A Note on the Steady High-Reynolds-Number Flow About a Circular Cylinder, *J. Fluid Mech.* **157** (1985) 493–500.
31. M. Poliashenko and C.K. Aidun, A Direct Method for Computation of Simple Bifurcations, *Journal of Computational Physics* **121** (1995) 246–260.
32. A.K. Prasad and J.R. Koseff, Reynolds Number and End-Wall Effects on a Lid-Driven Cavity Flow, *Phys. Fluids A* **1** (1989) 208–218.
33. N. Ramanan and G.M. Homsy, Linear Stability of Lid-Driven Cavity Flow, *Phys. Fluids* **6** (1994) 2690–2701.
34. M. Sahin and R.G. Owens, A Novel Fully-Implicit Finite Volume Method Applied to the Lid-Driven Cavity Flow Problem. Part II. Linear Stability Analysis, *Int. J. Numer. Methods Fluids* **42** (2003) 79–88.
35. H. Schlichting and K. Gersten, *Boundary Layer Theory* (8th revised and enlarged edn), Springer, 2000.
36. R. Schreiber and H.B. Keller, Driven Cavity Flows by Efficient Numerical Techniques, *J. Comp. Physics* **49** (1983) 310–333.
37. P.N. Shankar and M.D. Deshpande, Fluid Mechanics in the Driven Cavity, *Annu. Rev. Fluid Mech.* **32** (2000) 93–136.
38. F.T. Smith, A Structure for Laminar Flow Past a Bluff Body at High Reynolds Number, *J. Fluid Mech.* **155** (1985) 175–191.
39. J.S. Son and T. Hanratty, Numerical Solution for the Flow Around a Cylinder at Reynolds Numbers of 40, 200 and 500, *J. Fluid Mech.* **35** (1969) 369–386.
40. J.C. Tennehill, D.A. Anderson and R.H. Pletcher, *Computational Fluid Mechanics and Heat Transfer* (2nd edn), Taylor & Francis, 1997.
41. G. Tiesinga, F.W. Wubs and A.E.P. Veldman, Bifurcation Analysis of Incompressible Flow in a Driven Cavity by the Newton-Picard method, *Journal of Computational and Applied Mathematics* **140** (2002) 751–772.
42. S-Y. Tuann and M.D. Olson, Numerical Studies of the Flow Around a Circular Cylinder by a Finite Element Method, *Computers and Fluids* **6** (1978) 219–240.
43. D.C. Wan, Y.C. Zhou and G.W. Wei, Numerical Solution of Incompressible Flows by Discrete Singular Convolution, *Int. J. Numer. Methods Fluids* **38** (2002) 789–810.
44. E. Weinan and L. Jian-Guo, Vorticity Boundary Condition and Related Issues for Finite Difference Schemes, *J. Comp. Physics* **124** (1996) 368–382.

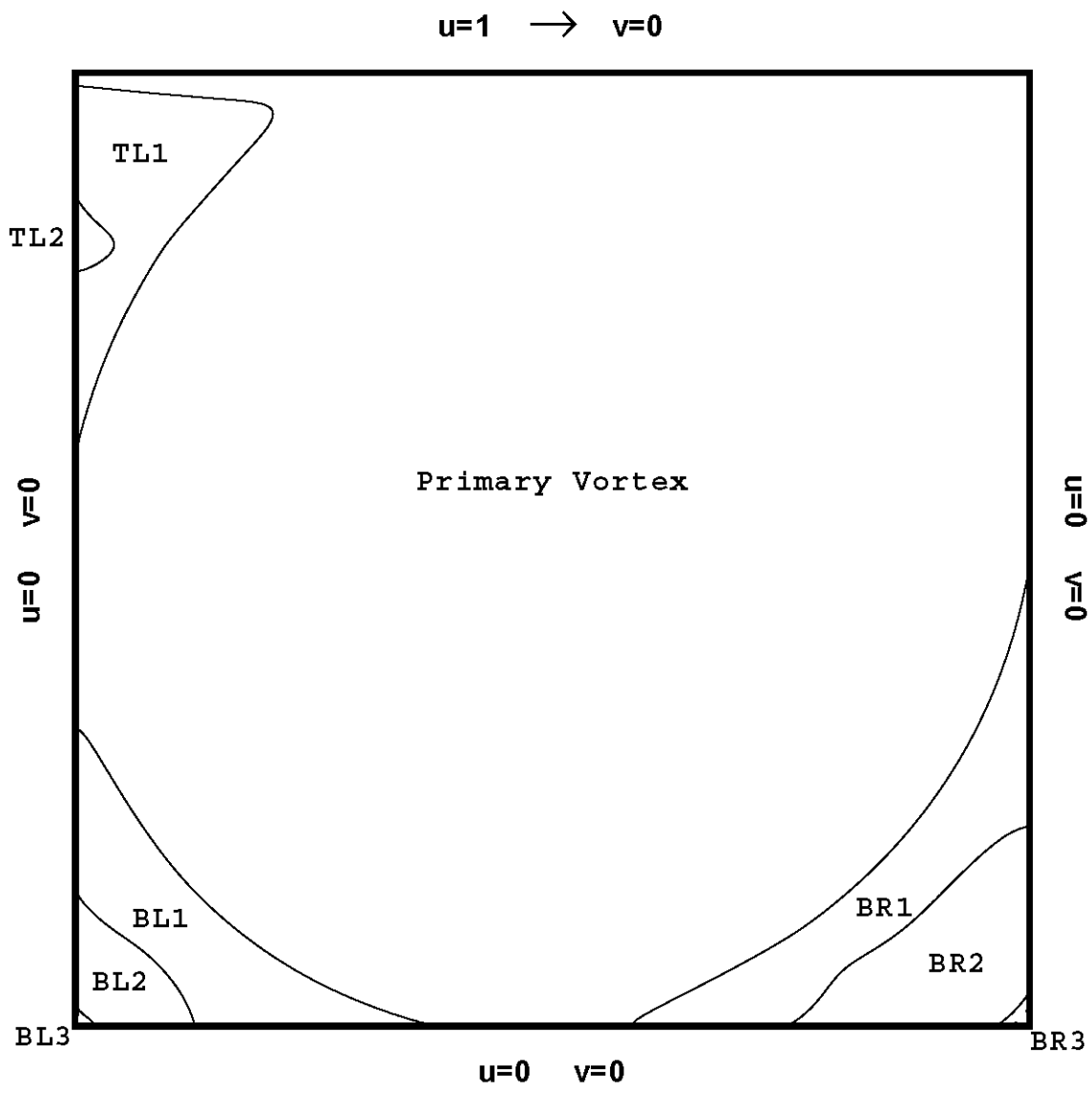
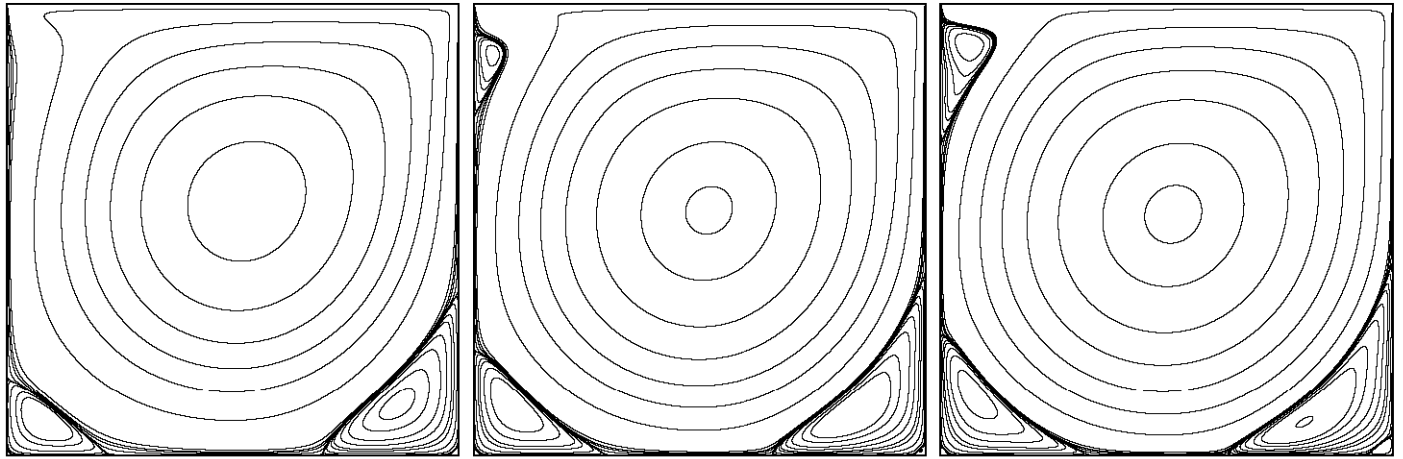


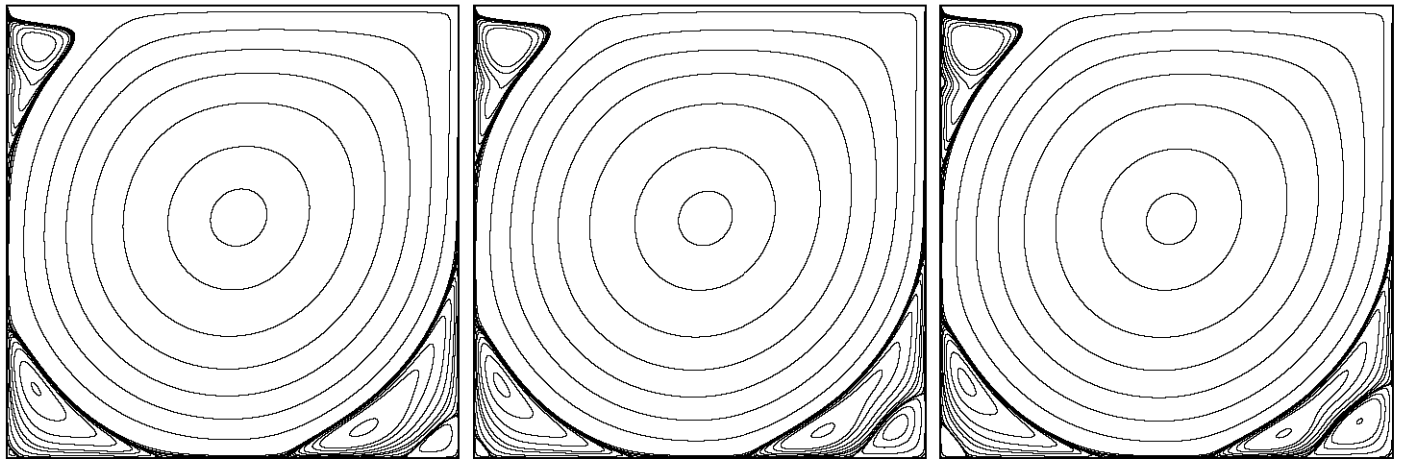
Figure 1. Schematic view of driven cavity flow



a) $Re=1,000$

b) $Re=2,500$

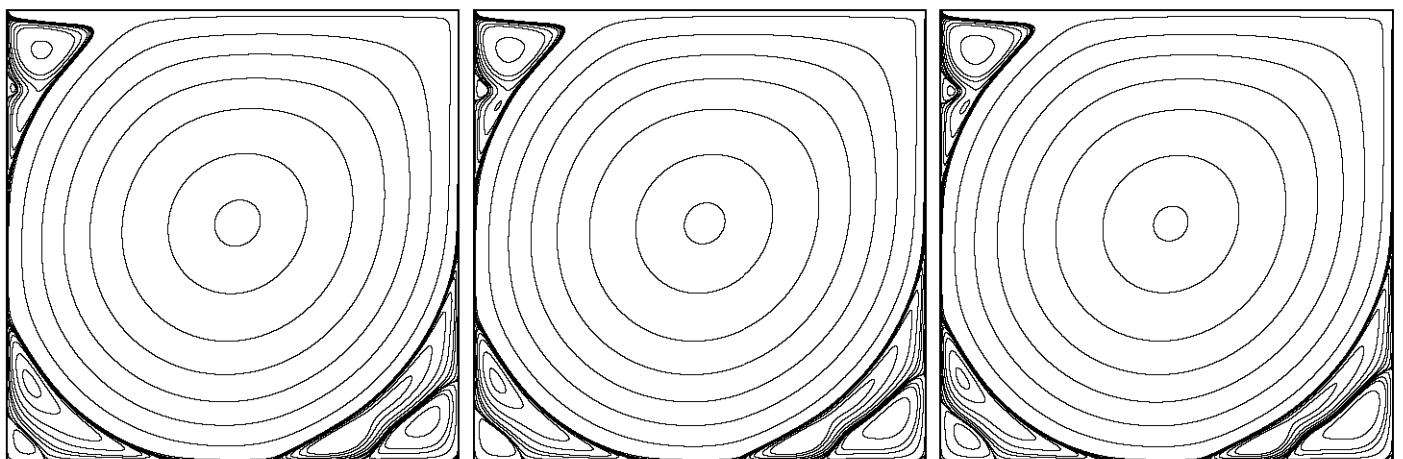
c) $Re=5,000$



d) $Re=7,500$

e) $Re=10,000$

f) $Re=12,500$

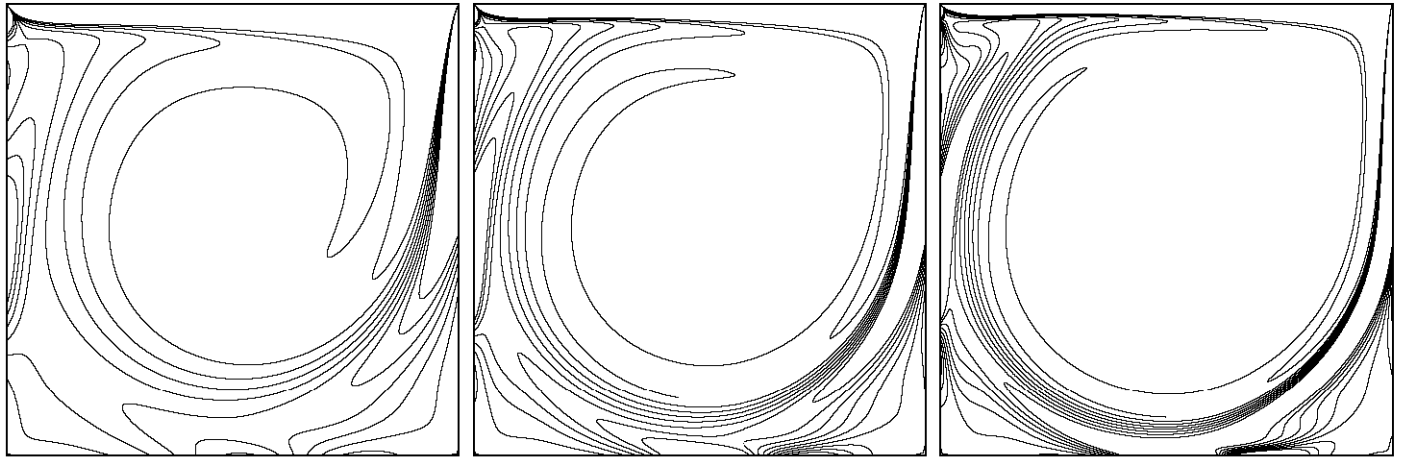


g) $Re=15,000$

h) $Re=17,500$

i) $Re=20,000$

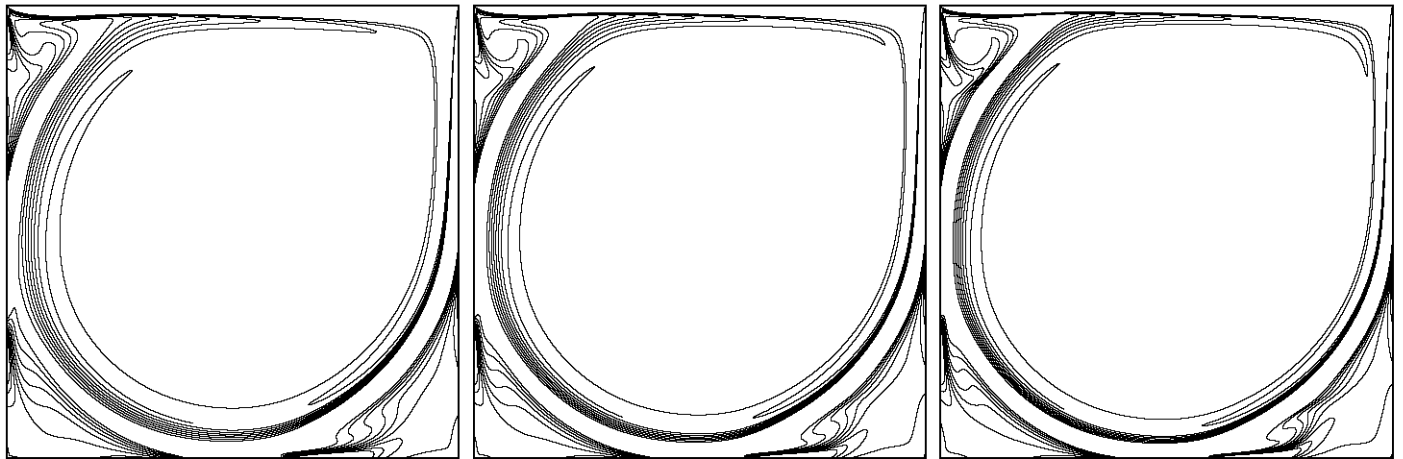
Figure 2. Streamfunction contours at various Reynolds numbers



a) $Re=1,000$

b) $Re=2,500$

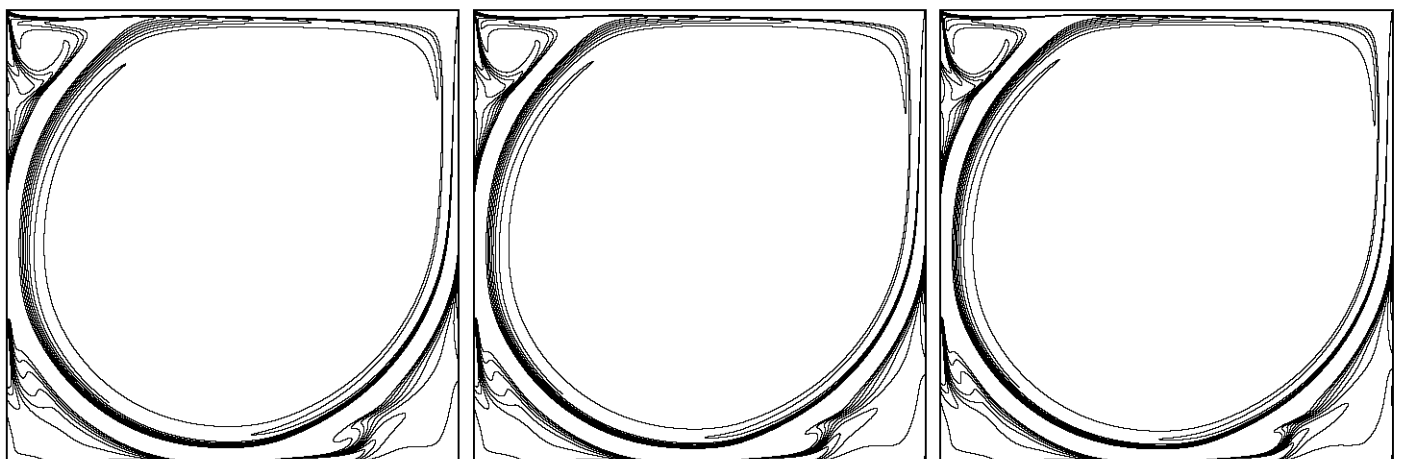
c) $Re=5,000$



d) $Re=7,500$

e) $Re=10,000$

f) $Re=12,500$



g) $Re=15,000$

h) $Re=17,500$

i) $Re=20,000$

Figure 3. Vorticity contours at various Reynolds numbers

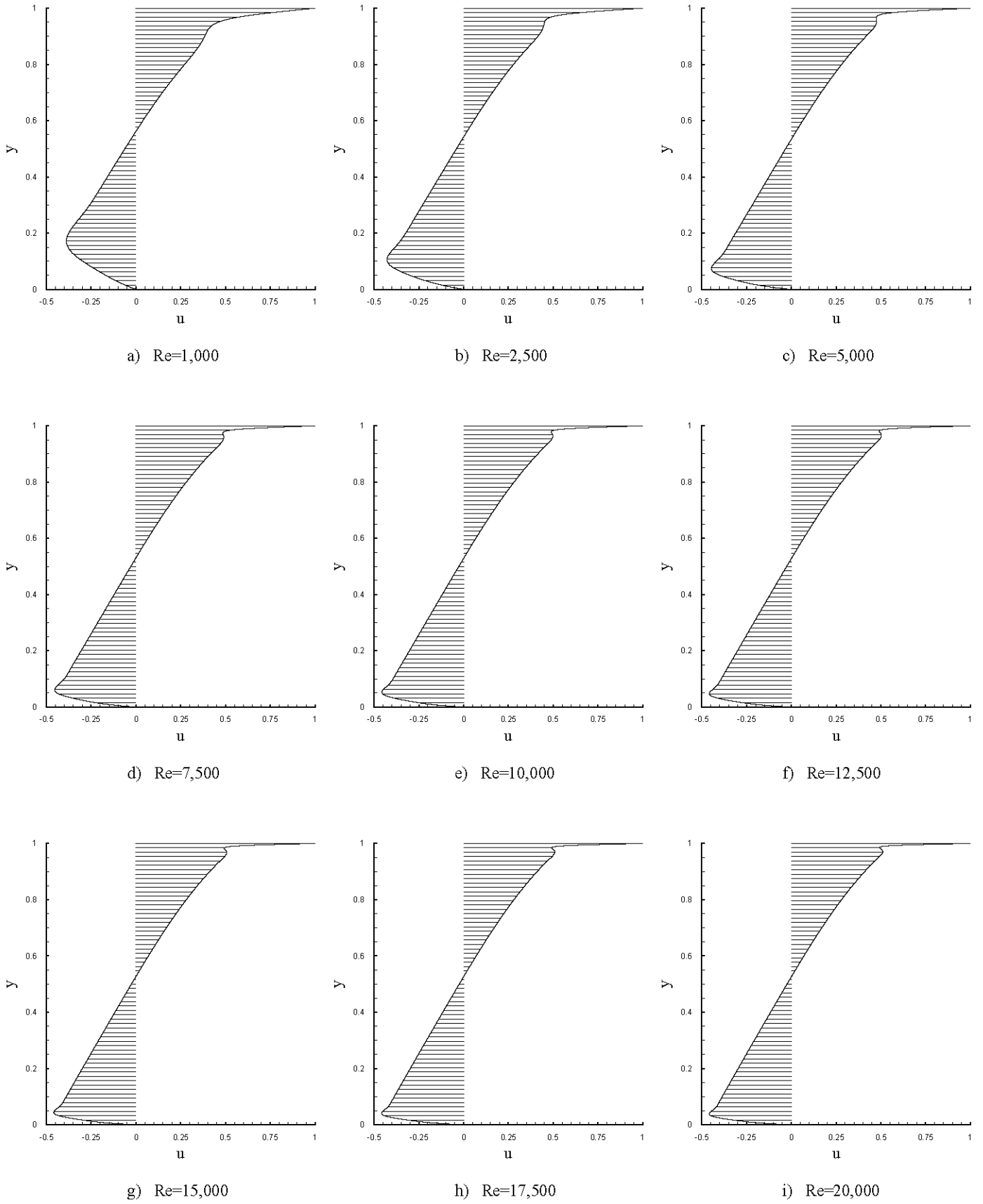


Figure 4. The u -velocity profiles along a vertical line passing through the center of the cavity

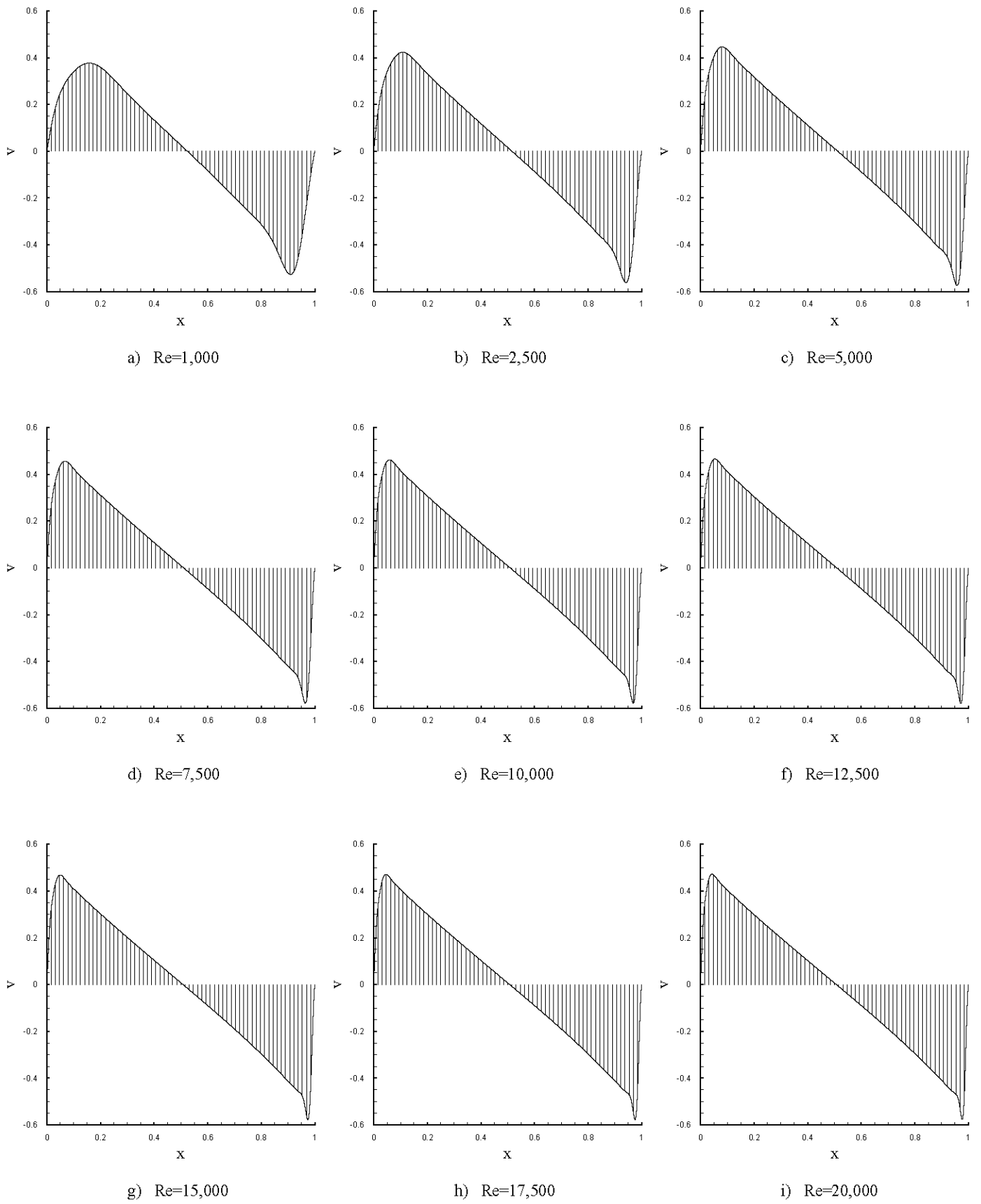


Figure 5. The v -velocity profiles along a horizontal line passing through the center of the cavity

Re	β
1000	1.2
2500	1.0
5000	0.8
7500	0.6
10000	0.5
12500	0.5
15000	0.4
17500	0.3
20000	0.3

Table 1. The relaxation parameter, β , used in SOR at various Reynolds numbers for 1025×1025 grid mesh

		Re	1000	2500	5000	7500	10000	12500	15000	17500	20000
Primary Vortex	ψ	-0.118888	-0.121337	-0.121942	-0.121939	-0.121781	-0.121571	-0.121342	-0.121105	-0.120865	
	ω	-2.067052	-1.974087	-1.936291	-1.920053	-1.909677	-1.901830	-1.895353	-1.889712	-1.884630	
	(x, y)	(0.5313, 0.5654)	(0.5195, 0.5439)	(0.5146, 0.5352)	(0.5137, 0.5322)	(0.5117, 0.5303)	(0.5107, 0.5283)	(0.5107, 0.5283)	(0.5098, 0.5273)	(0.5098, 0.5264)	
BR1	ψ	0.17287E-02	0.26594E-02	0.30677E-02	0.32198E-02	0.31846E-02	0.30930E-02	0.29991E-02	0.29019E-02	0.28038E-02	
	ω	1.111550	1.923505	2.720926	3.216140	3.751749	4.335619	4.938041	5.504286	6.080160	
	(x, y)	(0.8643, 0.1123)	(0.8350, 0.0908)	(0.8057, 0.0732)	(0.7910, 0.0654)	(0.7754, 0.0596)	(0.7607, 0.0547)	(0.7471, 0.0498)	(0.7354, 0.0469)	(0.7246, 0.0439)	
BL1	ψ	0.23314E-03	0.92939E-03	0.13729E-02	0.15308E-02	0.16118E-02	0.16585E-02	0.16730E-02	0.16587E-02	0.16298E-02	
	ω	0.350476	0.980549	1.510725	1.868003	2.145982	2.320998	2.507351	2.692707	2.932753	
	(x, y)	(0.0830, 0.0781)	(0.0840, 0.1113)	(0.0732, 0.1367)	(0.0645, 0.1523)	(0.0586, 0.1621)	(0.0557, 0.1670)	(0.0527, 0.1719)	(0.0508, 0.1768)	(0.0479, 0.1826)	
BR2	ψ	-0.50156E-07	-0.12139E-06	-0.14045E-05	-0.31991E-04	-0.13770E-03	-0.25203E-03	-0.33722E-03	-0.40202E-03	-0.45797E-03	
	ω	-0.89202E-02	-0.12542E-01	-0.34116E-01	-0.156359	-0.302428	-0.398521	-0.464422	-0.518223	-0.559633	
	(x, y)	(0.9922, 0.0078)	(0.9902, 0.0088)	(0.9785, 0.0186)	(0.9521, 0.0420)	(0.9355, 0.0674)	(0.9277, 0.0811)	(0.9268, 0.0889)	(0.9287, 0.0967)	(0.9307, 0.1045)	
BL2	ψ	-0.63952E-08	-0.27624E-07	-0.66119E-07	-0.20023E-06	-0.10866E-05	-0.64356E-05	-0.22641E-04	-0.49966E-04	-0.82094E-04	
	ω	-0.27286E-02	-0.62456E-02	-0.99654E-02	-0.14650E-01	-0.31184E-01	-0.74967E-01	-0.140378	-0.200096	-0.250093	
	(x, y)	(0.0049, 0.0049)	(0.0059, 0.0059)	(0.0078, 0.0078)	(0.0107, 0.0117)	(0.0166, 0.0205)	(0.0264, 0.0322)	(0.0381, 0.0420)	(0.0498, 0.0488)	(0.0586, 0.0547)	
TLL1	ψ	-	0.34320E-03	0.14442E-02	0.21247E-02	0.26129E-02	0.29797E-02	0.32676E-02	0.35027E-02	0.37012E-02	
	ω	-	1.315587	2.074175	2.231256	2.297052	2.350284	2.399048	2.437302	2.469855	
	(x, y)	-	(0.0430, 0.8896)	(0.0635, 0.9092)	(0.0664, 0.9121)	(0.0703, 0.9111)	(0.0742, 0.9111)	(0.0771, 0.9111)	(0.0791, 0.9121)	(0.0801, 0.9121)	
BR3	ψ	-	-	0.42980E-10	0.84067E-09	0.38803E-08	0.76029E-08	0.11513E-07	0.17251E-07	0.26758E-07	
	ω	-	-	0.11263E-03	0.14869E-02	0.21783E-02	0.35141E-02	0.41508E-02	0.45564E-02	0.55315E-02	
	(x, y)	-	-	(0.9990, 0.0010)	(0.9971, 0.0029)	(0.9961, 0.0039)	(0.9951, 0.0049)	(0.9951, 0.0059)	(0.9941, 0.0059)	(0.9932, 0.0068)	
BL3	ψ	-	-	-	0.80824E-11	0.40286E-10	0.17663E-09	0.59435E-09	0.14160E-08	0.22569E-08	
	ω	-	-	-	0.29106E-03	0.14243E-03	0.75527E-03	0.10105E-02	0.14427E-02	0.18191E-02	
	(x, y)	-	-	-	(0.0010, 0.0010)	(0.0010, 0.0010)	(0.0020, 0.0020)	(0.0020, 0.0020)	(0.0029, 0.0029)	(0.0039, 0.0029)	
TLL2	ψ	-	-	-	-	-	-0.14694E-05	-0.15063E-04	-0.39746E-04	-0.68864E-04	
	ω	-	-	-	-	-	-0.219588	-0.506032	-0.758492	-0.941342	
	(x, y)	-	-	-	-	-	(0.0068, 0.8311)	(0.0146, 0.8262)	(0.0205, 0.8223)	(0.0244, 0.8203)	

Table 2. Properties of primary and secondary vortices; streamfunction and vorticity values, (x, y) locations

Re	$Q_1 = \frac{ \int_0^1 u dy }{Q_c}$	$Q_2 = \frac{ \int_0^1 v dx }{Q_c}$
1000	2.451×10^{-10}	4.741×10^{-11}
2500	1.611×10^{-9}	2.550×10^{-10}
5000	5.625×10^{-9}	7.018×10^{-10}
7500	1.034×10^{-8}	9.813×10^{-10}
10000	1.411×10^{-8}	8.834×10^{-10}
12500	1.547×10^{-8}	2.795×10^{-10}
15000	1.313×10^{-8}	9.115×10^{-10}
17500	5.872×10^{-9}	2.743×10^{-9}
20000	7.364×10^{-9}	5.252×10^{-9}

Table 3. Volumetric flow rates through a vertical line, Q_1 , and a horizontal line, Q_2 , passing through the geometric center of the cavity